Neurogenesis and astrogenesis contribute to vestibular compensation in the neurectomized adult cat: cellular and behavioral evidence

Sophie Dutheil, Jean Michel Brezun, Jacques Leonard, Michel Lacour, Brahim Tighilet

UMR 6149 "Neurobiologie Intégrative et Adaptative"
Pôle 3C « Comportement, Cerveau, Cognition », Centre de St Charles – Case B – 3 Place Victor Hugo, 13331 Marseille Cedex 3 – France

Figures: 7; Tables: 1; words in abstract: 135; in introduction: 550; in discussion: 1340

Correspondence to: Dr. Brahim Tighilet, UMR 6149 Université de Provence/CNRS "Neuroscience Intégrative et Adaptative"Pôle 3C « Comportement, Cerveau, Cognition », Centre de St Charles – Case B – 3 Place Victor Hugo, 13331 Marseille Cedex 3 – France. Phone: (33)0488576841; Fax: (33)0488576818; E-mail: brahim.tighilet@univ-provence.fr

Abstract

Neurogenesis occurs in some regions of the adult mammalian brain and gives rise to neurons integrated into functional networks. In pathological or postlesional conditions, neurogenesis and astrogenesis can also occur, as demonstrated in the deafferented vestibular nuclei after unilateral vestibular neurectomy in the adult cat. Here we report that in cats infused with an antimitotic drug, cytosine-ß-D arabinofuranoside (AraC), the number of GAD67 and GFAP immunoreactive cells is increased, despite the total mitotic activity blockade observed in the deafferented vestibular nuclei after unilateral vestibular neurectomy. At the behavioral level, recovery of posturo-locomotor function was drastically delayed, and no alteration of the horizontal spontaneous nystagmus was observed. These cellular and behavioral results suggest that reactive neurogenesis and astrogenesis might contribute highly to vestibular compensation in the adult cat, probably by accelerating the recovery of vestibular functions.

Key words: adult neurogenesis, GABA, GFAP, vestibular compensation, vestibular nuclei complex, AraC

INTRODUCTION

Adult neural stem progenitors reside in many areas of the adult mammalian central nervous system (CNS), but continuous neurogenesis occurs only in two restricted regions: in the subgranular zone (SGZ) of the dentate gyrus (DG) of the hippocampus and in the subventricular zone (SVZ) of the lateral ventricles[1]. Among the interrogations raised by this new form of adult plasticity is the function of these new neurons[2]. *In vitro* experiments in rodents have shown that new DG or SVZ neurons develop electrophysiological and synaptic properties very similar to and even indistinguishable from mature neurons[3-6]. Spontaneous neurogenesis leads to functional integration, into pre-existing neural networks, of the cells newly generated in the DG[7,8] and in the olfactive bulb[6,9]. These cells become active and contribute to the transmission of information in the brain. In response to physiological or pathological stimulations, newborn DG and SVZ neurons express the immediate early gene product c-Fos, a neural activity marker[10,11]. These data suggest that neurons elaborated during adulthood in delimited zones of the CNS can integrate pre-established neural networks and participate actively in their function. Outside these two discrete areas, proliferating cells give rise to glia but not neurons in the intact adult CNS. However, in pathological or injured states of the brain, neurogenesis and gliogenesis have been reported both in known neurogenic zones and in other areas[12,13], such as the dorsal vagal complex or the vestibular nuclei (NV). In the dorsal vagal complex the number of newly generated neurons and microglial cells increases after unilateral vagotomy in the adult rat[14]; in the vestibular nuclei, astroglial and microglial reactions occur after unilateral removal of vestibular and cochlear receptors[15,16]. Together, these results suggest that the adult mammal CNS is able to generate the main characteristic cell types of nervous tissue (neurons, astrocytes and microglial cells) for brain restructuring and to integrate them in pre-established networks. But the functional benefit of this form of structural plasticity remains poorly documented.

We have previously demonstrated in the adult cat that unilateral vestibular neurectomy (UVN)[17] causes an intense reactive cell proliferation in the deafferented vestibular nuclei (VN). Most of these new cells survive one month after injury and give rise to astrocytes, microglial cells, and neurons. The newly generated neurons express a GABAergic phenotype and might correspond morphologically to intrinsic commissural neurons, local vestibular interneurons, or to groups II, III, or IV, representing the vestibulo-ocular, vestibulo-olivary, and vestibulo-spinal neurons, respectively[18]. The question raised in the present study is whether reactive astrogenesis and GABAergic neurogenesis contribute functionally to vestibular compensation - i.e. the postlesional restoration of the impaired vestibular functions observed in various animal models[19]. To determine if reactive cell proliferation plays a functional role in the vestibular compensation process, the mitotic activity of the dividing new cells was blocked by a continuous infusion of cytosine-ß-D arabinofuranoside (AraC, S-phase-specific antimitotic drug) in the fourth ventricle. To determine whether delayed AraC infusion had an incidence on vestibular compensation, the drug was administered to adult cats either immediately after being submitted to UVN or 3 weeks after UVN, when all the newly generated cells have been formed. Cell division blockage and its consequences were characterized at the cellular level with BrdU, GAD67, and GFAP immunostainings. Repercussions of AraC infusion on the behavioral recovery processes were evaluated with oculomotor and posturo-locomotor tests.

RESULTS

AraC infusion blocks cell proliferation

Using 5-bromo-2'deoxyuridine (BrdU) injected 3 hours before the adult cats were killed by perfusion, we examined the cells newly generated in the vestibular nuclei and the subventricular zone. A very low level of BrdU-immunoreactive (Ir) cells was observed in the vestibular nuclei (VN) complex and around the subependimary layer of the fourth ventricle of control cats, as previously described in this model[17] [medial vestibular nuclei (MVN), 19 ± 1.93; inferior vestibular nuclei (IVN), 33.19 ± 2.02; lateral vestibular nuclei (LVN) 24.5 ± 1.93; superior vestibular nuclei (SVN), 23.75 ± 2.55)]. In contrast, a significantly high number of BrdU-Ir cells was found in the SVZ of these animals, with a mean value of 2902.5 ± 82.3.

During vestibular compensation, we aimed to characterize the functional role of the reactive cells generated after UVN. Cell proliferation was blocked using AraC delivered in the vicinity of vestibular nuclei. Consistent with a previous report on adult UVN cats[17], we found a strong ratio of surviving BrdU-Ir cells in all the deafferented VN when UVN was coupled with a continuous infusion of sodium chloride (NaCl) during 30 days (**Fig. 1 a**,**b**). We found an increase in BrdU immunoreactivity, showing a multiplying factor of 2700 to 6250 according to the homologous VN (MVN, 843.74 ± 25.5; IVN, 1044.0 ± 22.83; LVN, 1530.37 ± 11.33; SVN, 648.75 ± 31.93). NaCl did not influence the rate of cell proliferation in UVN cats and could therefore be considered as innocuous. In contrast, the number of BrdU-Ir nuclei in the VN was close to zero in cats infused with the antimitotic drug immediately after UVN (UVN/AraC $D_{0\text{-}30}$ group), thus confirming the efficacy of AraC. AraC blocked the cell proliferation in the whole VN.

In cats submitted from the twentieth to the fiftieth day ($D_{20\text{-}50}$) to NaCl or to AraC infusion, the number of BrdU-Ir cells in the VN was similar to that of the UVN cats infused

early with NaCl (UVN/NaCl $D_{0\text{-}30}$), see **Fig. 1 a**,**b**. Delayed infusion had no incidence on cell proliferation, and training the cats on the rotating beam did not influence the rate of cell proliferation in the VN (data not shown).

Furthermore, neither the UVN nor the AraC infusion in the fourth ventricle affected BrdU immunoreactivity in the SVZ (**Fig. 2 a**,**b**). The total number of BrdU-Ir nuclei in the SVZ of the UVN/AraC $D_{0\text{-}30}$ (3115.83 ± 97.37) remained similar to the controls or to the UVN/NaCl $D_{0\text{-}30}$ cats (2902.5 ± 82.31 and 2896.66 ± 99.35 respectively). This finding indicates that AraC acts selectively and blocks local reactive cell proliferation only if the infusion occurs early after UVN.

AraC infusion decreases the number of GFAP-immunoreactive cells

To determine the effect of UVN on reactive astrogenesis in the VN, immunohistochemical staining was carried out on brainstem sections at 30 days post-vestibular axotomy. GFAP-Ir cells detected in the VN of the five groups of cats are presented in **Fig. 3a**. GFAP-Ir cells, characterized by richly branched cells with translucent cytoplasm, were sparse in the control group and became further conspicuous in the deafferented VN of UVN cats submitted to early NaCl infusion. The control group exhibited a relatively high number of GFAP-Ir cells in all the VN (MVN, 35469.58 ± 536.62; IVN, 27772.35 ± 970.97; LVN 40872.58 ± 495.71; SVN, 41041.3 ± 454.75), see **Fig. 3b**. After UVN, a strong astroglial reaction was observed on the deafferented VN only. In the UVN/NaCl $D_{0\text{-}30}$ group, the numbers of astrocytes were 109428.6 ± 1035.87 in the MVN, 70191.2 ± 1949.8 in the IVN, 79470.3 ± 1808.3 in the LVN, 131160.5 ± 1199.04 in the SVN. Infusion of AraC from $D_{0\text{-}30}$ in UVN cats significantly decreased GFAP immunoreactivity in the deafferented VN as compared to the UVN/NaCl $D_{0\text{-}30}$ group ($P = 0.0001$). However, the total number of GFAP-Ir cells in each deafferented VN of this AraC group remained significantly higher than for the control group ($P = 0.0001$). The

astroglial reaction observed in the UVN cats infused with NaCl or AraC from D_{20} to D_{50} was similar to that observed in the NaCl $D_{0\text{-}30}$ group. These data suggest that delayed infusion had no incidence on GFAP-immunoreactivity. The double immunohistochemical labeling (GFAP versus BrdU) showed newly generated GFAP-Ir cells only in the UVN/NaCl $D_{0\text{-}30}$ group (**Fig. 4 a-c**); no co-localization of these two markers was detected in the UVN/AraC $D_{0\text{-}30}$ group (**Fig. 4 d-f**).

AraC infusion decreases the number of GABAergic neurons

To clarify whether, after UVN, AraC affects GABA-immunoreactivity in the VN, the number of GAD67 immunopositive neurons was quantified in the different groups by the optical fractionator method[20]. The number of GAD67-Ir neurons was moderate and symmetric in both sides of the VN in the control group. The mean data for these animals were 98.48 ± 7.91 in the MVN, 82.65 ± 5.01 in the IVN, 108.46 ± 5.90 in the LVN, and 69.12 ± 4.02 in the SVN. In contrast, UVN significantly increased the number of GAD67-Ir neurons in the deafferented MVN, IVN, and LVN, whatever the vestibular-neurectomized groups compared to the control group ($P = 0.0001$). No changes were observed in the SVN. In the UVN/NaCl $D_{0\text{-}30}$ group, the values were 293.62 ± 14.68 in the MVN, 161.9 ± 5.2 in the IVN, 198.85 ± 8.62 in the LVN, and 72.45 ± 5.88 in the SVN (**Fig. 5 a**,**b**). Despite the lack of the reactive cell proliferation in the VN under early AraC infusion from D_0 to D_{30}, a significant increase in the number of GAD67-Ir neurons was still observed in the deafferented VN, relative to the control group ($P = 0.0001$). The number of GAD-Ir neurons in the UVN/AraC $D_{0\text{-}30}$ remained significantly lower than in the other UVN groups of cats for the MVN, IVN, and LVN (**Fig. 5 b**). Double immunohistochemical labeling (GAD67 and BrdU) showed newly generated GAD67-Ir neurons only in the UVN/NaCl $D_{0\text{-}30}$ group (**Fig. 4 g-i**); no co-localization of these two markers was detected in the UVN/AraC $D_{0\text{-}30}$ group (**Fig. 4 j-l**).

AraC infusion has no incidence on the horizontal spontaneous nystagmus (HSN)

For nystagmus recordings, cats were placed on an apparatus with their heads fixed, thus maintaining the horizontal semi-circular canals in the horizontal plane. The frequency of HSN was recorded by a camera and measured in the light as the number of quick phase beats towards the contralateral side relative to UVN in 10 sec (five repeated measures per animal per sampling time). The variance analysis (ANOVA) did not demonstrate significant effects depending on the groups, the postoperative time, or the interaction between these two factors. Immediately after UVN, animals showed an HSN that disappeared progressively. One day after UVN, the frequency of HSN in all the groups was between 14 and 16 beats per 10 seconds and declined progressively to disappear totally at the 8-day postlesion delay whatever the groups (**Fig. 6 a**). The AraC infusion did not alter the HSN, which fully recovered in UVN cats infused with AraC or with NaCl.

AraC infusion delays the posture function recovery

Static posture recovery was evaluated by measuring the surface delimited by the four legs of cats. Significant effects appeared depending on the groups ($P = 0.0001$), the postoperative time ($P = 0.0001$), and the interaction between these two factors ($P = 0.0001$). As a rule, the UVN cats infused with NaCl and those infused with AraC after a 20-day delay recovered similarly and did not differ from control UVN cats without any infusion. These three groups of cats regained a normal support surface 7 weeks after vestibular nerve transection. Conversely, the recovery of the UVN/AraC $D_{0\text{-}30}$ group was strongly delayed. **Fig. 6 b** shows the time course of posture function recovery in UVN cats infused with AraC or with NaCl. The UVN/AraC $D_{0\text{-}30}$ group exhibited significantly higher values (5.5 ± 0.38) than the UVN/NaCl $D_{0\text{-}30}$ group (5.0 ± 0.3) at 1 day post-UVN. The support surface reached control

values at 50 days post-UVN in the NaCl D_{0-30} group while it remained significantly large in the AraC D_{0-30} group (3.75 ± 0.03; $P = 0.0001$). The complete compensation of this parameter by the D_{0-30} AraC group was drastically delayed; it required 86 days. When AraC was infused from D_{20-50} after UVN, the recovery profile of the posture function was similar to that of the NaCl D_{0-30} group. These results suggest that early AraC infusion has an incidence on the support surface recovery.

AraC infusion delays locomotor balance recovery

Figure 6 c illustrates the mean development of the posturo-locomotor function in the cats infused or not with AraC during the preoperative conditioning period. Animals were conditioned to cross over the rotating beam, whose velocity was progressively increased. At one-day post-UVN, all animals fell on the deafferented side, and they were unable to walk on the rotating beam up to 8 days after vestibular deafferentation. As for posture recovery, the variance analysis (ANOVA) of the locomotor balance recovery demonstrated significant effects depending on the groups ($P = 0.0001$), the postoperative time ($P = 0.0001$), and the interaction between these two factors ($P = 0.0001$). Cats of the NaCl group crossed over the beam at the highest speed (100% Max P) at 46 days post-UVN. At this time, the AraC D_{0-30} cats were able to walk on only the immobile beam. The Max P of this group was strongly delayed (about 3 times more) and was reached at 146 days post-UVN. When AraC was infused from D_{20-50} after lesion, the recovery profile of the locomotor balance function was similar to that of the UVN cats submitted to an early NaCl infusion (**Fig. 6 d**). This result suggests that the delayed Max P performance under AraC infusion is not imputable to the nature of the drug. Recovery of locomotor balance (Max P) was complete in UVN cats infused with AraC or with NaCl, but it was strongly delayed in the AraC group when infusion was continuously done early from D_0 to D_{30}. In summary, when AraC is infused immediately

after UVN, only posturo-locomotor function recovery is delayed whereas the spontaneous horizontal nystagmus recovery remains comparable to that of the NaCl-infused group. Moreover, delayed AraC infusion has no effect on behavioral processes.

DISCUSSION

This study shows that AraC infusion had no incidence on horizontal spontaneous nystagmus (HSN) compensation. The disappearance of HSN may be explained by ocular fixation, a behavioral strategy used to block the spontaneous nystagmus. Mammals stabilize their gaze using their fovea: this ocular fixation process can therefore be used by the feline with their pseudo-fovea. In addition, the SVN, which is the structure most involved in oculomotor function, does not exhibit neurogenesis[17] and could thus require other plasticity mechanisms for compensation.

Whereas posturo-locomotor recovery of cats infused with NaCl or with AraC 20 days after UVN reached control values 4 to 5 weeks after lesion, precocious AraC cell proliferation blockage (UVN/AraC $D_{0\text{-}30}$) markedly delayed the recovery of postural and locomotor balance. For this group, the postural function was compensated at 3 months while the locomotor balance function was recovered later (5 months); for the other groups 1.5 month was required for both functions. A high number of newborn neurons were observed in the NVM, LVN, and IVN, which are mainly associated with static and dynamic postural functions[21]. This finding supports the notions that reactive cell proliferation contributes to restoration of the posturo-locomotor functions and that, since functional recovery is strongly delayed but complete after an early local AraC infusion, other compensatory mechanisms are involved. Thus, the functional recovery of these animals is not only dependent on neurogenesis and gliogenesis but it also requires other subprocesses at different levels. Different plasticity mechanisms underlying vestibular compensation have already been

described: molecular and neurochemical changes at pre- and postsynaptic levels of the VN cells[22,23], synaptic plasticity[24], sprouting of axon collaterals[25], and astroglial and microglial reactions[15,16]. Similar findings in mice showed that, after unilateral labyrinthectomy, the blockade of BDNF expression induced by infusion of antisense oligonucleotides in the VN specifically delays the compensation of postural deficits without incidence on ocular nystagmus[26]. Interestingly, the peak of BrdU positive cells 3 days after UVN in the deafferented VN[17] is correlated with a peak of BDNF and nerve growth factor (NGF) Ir-cells[27], suggesting that, in this model, neurotrophins secreted by both neurons and glial cells could modulate cell proliferation, survival, and differentiation[28]. Besides, Gliddon et al.[29] demonstrated in the guinea pig that chronic infusion of $GABA_A$ receptor antagonist in the deafferented VN specifically modified the expression of postural syndromes and not oculomotor ones, yet without incidence on their compensation rate. These data combined with ours strongly indicate that compensation of the HSN and posturo-locomotor functions would be governed by different processes[30] and that astrogenesis, neurogenesis, and neurotrophin or neuromediator expression in the VN complex may participate in their recovery.

In physiological conditions, astrocytes play a crucial role in ionic homeostasis and the maintenance of an ideal environment for neuronal cell function, participating in clearance and metabolism of neurotransmitters like glutamate in the extracellular space and regulating extracellular pH and levels of potassium[31,32]. Astrocytes also release various gliotransmitters such as glutamate, ATP, adenosine, D-serine, cytokines, BDNF, and NGF, and they proceed actively on adjacent neurons, glial cells, and blood vessels[33]. The increased number of GFAP-Ir cells observed in the deafferented VN might enhance the release of these various gliotransmitters in the extracellular space in order to locally favor neuronal survival, differentiation, excitability, or cell proliferation. Besides their neuronal implication on VN functional and structural reorganization, these findings lead us to speculate that astrocytes

might contribute highly to structural plasticity mechanisms and probably accelerate the recovery of vestibular functions.

The prevalent response to brain injury is reactive gliosis, which leads to hypertrophy of astrocytes and to upregulation of GFAP[34]. As previously observed[17], the UVN cats infused with NaCl showed a strong reactive GFAP-immunoreactivity in the deafferented VN. Similar findings have been demonstrated after axotomy in the hypoglossal nucleus[35] and after unilateral inner ear lesion in the vestibular and cochlear nuclei[36]. The increased number of GFAP-Ir cells could come in part from differentiation of the newly generated cells in the VN after UVN. They could also derive from mature astrocytes that retain developmental features, allowing dedifferentiation into other subtypes of astrocytes, neurons, or neural progenitors, as evidenced in the SVZ and in the hippocampus of mice[31,37]. Buffo and colleagues demonstrated that reactive astrocytes reacquired developmental stem cell properties and were a novel source of multipotent cells in the cortex after brain injury in the adult mouse[34]. In our model, the reactive astrogliosis in the deafferented VN was decreased in the AraC-infused group ($D_{0\text{-}30}$) but remained stronger than in the control group. This observation, combined with the total lack of BrdU-Ir nuclei in the deafferented VN, confirms the absence of newborn astrocytes after UVN in this group. The persistent astrogliosis observed in these animals might result from pre-existent astrocytes, upregulating GFAP protein expression after UVN and taking part in the neuroplasticity of the system after nerve transection. This notion is consistent with results of other authors who demonstrated that AraC treatment inhibited postlesional glial scar formation selectively after hypoglossal nerve transection in the rat. In addition, after AraC treatment following axotomy, astrocytes upregulated GFAP-Ir without ^{3}H-thymidine incorporation or BrdU immunostaining[38,39].

As in our previous experiments[40], the results presented here showed that, after UVN, a considerable amount of the cell proliferation observed in the deafferented VN differentiated

into GABAergic neurons. In contrast, in the deafferented VN of the AraC $D_{0\text{-}30}$ group, which did not exhibit BrdU-Ir cells, the increased number of GAD67-Ir neurons suggests that pre-existing neurons upregulated GAD67. These two plasticity mechanisms (GABA neurogenesis versus GAD67 upregulation) might occur in the deafferented VN in order to re-establish vestibular imbalance, which seems to be necessary for fine vestibular compensation. The GABAergic system is known to influence vestibular compensation[41], to rebalance electrical activity between the VN on both sides[22], and to control different steps of adult neurogenesis like differentiation[42,43]. The mechanism promoting neuronal and astroglial differentiation of the newly generated cells could implicate GABA inputs and $GABA_A$ receptors potentially located on neural stem cells[44]. It is known that GABAergic inputs to hippocampal progenitor cells promote activity-dependent neuronal differentiation[45] and regulate the synaptic integration of newly generated neurons in the adult brain[46]. Interestingly, we have previously observed a strong increase in GABA-staining varicosities in the deafferented VN complex after UVN in the cat[40], and it has been proposed that changes in GABA receptor function in the deafferented VN neurons act as a potent mechanism underlying vestibular compensation[47].

Numerous hypotheses can be postulated to clarify the functional significance of such GABAergic neurogenesis in vestibular function recovery. As previously evoked[17], newborn GABAergic neurons on the lesioned side could be inhibitory neurons directly acting on the contralateral excitatory neurons. Similarly, newborn GABAergic neurons could act on inhibitory mature neurons in the ipsilateral VN. Both mechanisms could contribute to attenuating the electrical asymmetry between the homologous VN. Another hypothesis concerns the effect of GABA on the VN neuron activity after UVN. GABA is known to elicit an excitatory signal in immature neurons and even in some mature neurons under specific or pathological conditions. The depolarizing or hyperpolarizing response depends on the Cl^-

gradient across the cell membrane[48,49] and on the cation-chloride-cotransporters expressed by mature and newborn neurons. To clarify the functional role of GABA in our model, the nature of inhibitory versus excitatory action of GABA should be determined by further studies.

In conclusion, the current study provides cellular and behavioral evidence for adult reactive astrogenesis and neurogenesis that contribute to vestibular compensation in the adult cat. Microenvironments of neurogenic zones are thought to have specific permissive factors for the proliferation, the differentiation, and the integration of new cells[2]. In the intact brain, the vestibular complex seems not to deliver adequate cues to allow secondary neurogenesis, but after UVN, the local environment would express survival and optimal factors for new generated cells. The mature nervous system could recapitulate developmental process, leading new cells to survive, migrate, differentiate, and probably integrate existing neural circuitry required for fine vestibular compensation. Additional experiments will aim to specify the postlesional factors promoting this reactive vestibular astro-neurogenesis and to elucidate the role of GABAergic neurogenesis and astrogenesis in vestibular compensation.

MATERIALS AND METHODS

Animals and surgeries. Experiments were performed on 40 adult domestic cats (3-5 kg) obtained from the "Centre d'élevage du Contigné" (Contigné, France). All experiments were carried out in line with the Animals (scientific procedures) Act, 1986 and associated guidelines, the European Communities Council Directive of 24 November 1986 (86/609/EEC), and the National Institutes of Health guide for the care and use of laboratory animals (NIH publications No. 8023, revised 1978). Cats were housed in a large confined space with normal diurnal light variations and free access to water and food.

Animals were anesthetized with ketamine dihydrochoride (20 mg/kg, i.m, Rhône Poulenc, Mérieux, France), received analgesic (tolfenamic acid; 4 mg/kg, i.m; Vetoquinol, Lure, France) and were kept at physiological body temperature using a blanket. The vestibular nerve was sectioned at a postganglion level after mastoïdectomy, partial destruction of the bony labyrinth, and surgical exposure of the internal auditory canal. The classical postural, locomotor, and oculomotor deficits displayed by the animals in the days following UVN were used as criteria indicating the effectiveness of the vestibular nerve lesion. Completeness of UVN had already been assessed by histological procedures in previous studies[50].

For the implantation and use of osmotic minipumps containing cytosine-ß-D arabinofuranoside (AraC) or NaCl, a stainless steel cannula was implanted under anesthesia into the fourth ventricle of the brain and connected to a subcutaneous minipump (Alzet, Alza Corporation, Palo Alto, CA; flow rate 2.5 μl/h for 30 days). A midline incision was made through the skin and musculature in the back of the neck, and a cannula connected to plastic tubing was inserted between the dorsal wall of the brainstem and the ventral face of the cerebellum and then cemented with dental cement to the skull. The air in the system was removed by filling up with saline or AraC (diluted into a NaCl solution, 0.13 mM), after which the tubing was connected to an osmotic minipump, and the skin was incised. Cats (n =

34) were infused continuously into the cerebrospinal fluid of the fourth ventricle with an antimitotic agent, AraC, known to block cell proliferation in brain structures, or with NaCl, using the osmotic minipump.

Study design. To determine the functional role of the reactive cell proliferation occurring in the VN after UVN and its functional critical period, five groups of cats were used for both cellular and behavioral investigations: i) control that did not undergo UVN (*n* = 4), ii) UVN with early NaCl infusion (UVN/NaCl $D_{0\text{-}30}$, *n* = 8), iii) UVN with early AraC infusion (UVN/AraC $D_{0\text{-}30}$, *n* = 8), iv) UVN with delayed NaCl infusion (UVN/NaCl $D_{20\text{-}50}$, *n* = 8), v) UVN with late AraC infusion (UVN/AraC $D_{20\text{-}50}$, *n* = 8). In addition, to determine if AraC provided behavioral changes (conditioning on rotating beam, postural function and global sensorimotor activity) and/or side effects (salivation, vomiting), a group of non-lesioned cats (*n* = 2) underwent an infusion of AraC during the conditioning period (Non lesioned AraC group). Another group of non-lesioned cats (*n = 2*) was used for determining if the conditioning on rotating beam affects cell proliferation in the VN (conditioning control group). (See **Fig. 7**). Immunostaining analyses of postlesional cell proliferation and cell differentiation were performed in the VN and the subventricular zone (SVZ). The changes in behavioral recovery profile were analyzed with different behavioral tests (ocular horizontal nystagmus, support surface, and conditioning on rotating beam).

BrdU labeling and immunohistochemistry. Animals were injected with BrdU (200 mg/kg) and killed 27 (UVN $D_{0\text{-}30}$) or 47 (UVN $D_{20\text{-}50}$) days later (**Fig. 7**). The low doses administered to animals are not liable to generate side effects but are sufficient to mark the cells in S-phase synthesizing DNA (see[17]).

The cats were deeply anesthetized with ketamine dihydrochoride (20 mg/kg, i.m, Rhône Poulenc, Mérieux, France) and killed by paraformaldehyde perfusion. See Tighilet, Brezun et

al.[17] for details. Immunohistochemical labeling of BrdU-, GFAP-, and GAD67-immunoreative (Ir) cells was performed according to Tighilet, Brezun et al.[17]. Double immunofluorescent stained sections were incubated with GAD67 or GFAP combined with BrdU-Ir. The optimal antibody dilutions and staining procedures are described in **Table 1**. Differentiation of the newly generated cells was analyzed with double labeling analysis performed using confocal imaging with a Leica TCS SP2 laser scanning microscope equipped with a *63x/1.32 n.a.* oil immersion lens. The fields of view were then examined by confocal microscopy, and 1-μm-step Z series were obtained.

Spontaneous nystagmus recovery. The cat was placed on an apparatus with its head fixed and bent forward 23 deg, thus maintaining the horizontal semicircular canals in the horizontal plane. The frequency of the horizontal spontaneous nystagmus was recorded in the light using a video camera (Sony HDV) as the number of quick phase beats towards the contralateral side relative to UVN in 10 sec (five repeated measures per animal per sampling time).

Posture recovery. Posture deficits and recovery were evaluated by measuring the support surface delimited by the four legs of the cat standing erect at rest, without walking. The support surface can be regarded as a good estimate of postural control because it reflects the cat's behavioral adaptation compensating the static vestibulospinal deficits induced by the vestibular lesion. As a rule, the support surface was small in the normal cat (about 50-100 cm^2) and greatly increased in the days following unilateral vestibular lesion. To quantify the support surface, cats were placed in a device with a graduated transparent floor that allowed them to be photographed from underneath. Five repeated measurements were done for each cat tested at each postoperative time, and an average was calculated for each experimental session. The support surface was measured as the surface delimited by the four legs using an image analysis system (canvas, 9^{TM}, Deneba software, Miami, FL). Data recorded after

vestibular lesion were compared to prelesion values by using individual references, that is, each animal acted as its own control.

Equilibrium function recovery. Locomotor balance function was quantified using the rotating beam experimental device. Two compartments (0.5 x 0.6 x 0.5 m) were connected by a horizontal beam (length: 2 m; diameter: 0.12 m). The beam, placed 1.2 m off the ground, could be rotated along its longitudinal axis with a constant angular velocity ranging from 0° to 588,4 °/s (about more than 1.5 turn/s). The beam was equipped with a safety net to ensure the animals were protected in case of fall. Animal reward consisted of a small piece of fish (or meat) placed in a small bowl in the target compartment. Cats were conditioned to cross over the beam. First crossings were made on the immobile beam and, thereafter, on the rotating beam, whose velocity was progressively increased after four consecutive trials without fall. Equilibrium function was quantified by measuring the highest speed of beam rotation that did not induce a fall. This maximal rotation speed determined the maximal locomotor balance performance (Max P). Preoperative training on the rotating beam necessitated 6 to 10 training periods of 1 h per day, depending on the cats. Training was stopped when the cats' Max P was reached and stabilized at its highest level, which was found to be remarkably similar from one cat to another.

Cell counts and statistical analysis. The VN and the SZV were identified through Berman's stereotaxic atlases. BrdU-Ir was quantified for each VN (medial, inferior, lateral, and superior vestibular nuclei: MVN, IVN, LVN, and SVN, respectively) and for the SVZ. GFAP-Ir cells and GAD67-Ir neurons were analyzed in each VN on both sides (left/right: sham-operated cats; ipsilateral /contralateral: UVN-lesioned cats). The cell count was made with a Nikon microscope (Eclipse 80 i) equipped with a motorized X-Y-Z sensitive stage and a video

camera connected to a computerized image analysis system (Mercator; Explora Nova, La Rochelle, France). The total number of immunolabelled cells was estimated using the optical fractionator method[20]. For each labeling, the quantified sections were systematically selected with a size step of 480 μm along the anteroposterior axis. We counted only Ir-cells in focus within the height of the dissector (10 μm) and inside the limits of the counting frame without touching the forbidden lines. Accordingly, the statistical analysis was evaluated by ANOVA to test the effects of the group (NaCl or AraC), the side (deafferented vs intact), and the structure (MVN, IVN, LVN, SVN and SVZ) on BrdU-Ir, GFAP-Ir, and GAD67-Ir staining and to determine the interactions between these variables. ANOVA was followed by post-hoc analysis with the Scheffe test (stateview II, SAS software Inc., Cary, NC).

REFERENCES

1. Ming, G.L. & Song, H. Adult neurogenesis in the mammalian central nervous system. *Annu Rev Neurosci* **28**, 223-50 (2005).
2. Zhao, C., Deng, W. & Gage, F.H. Mechanisms and functional implications of adult neurogenesis. *Cell* **132**, 645-60 (2008).
3. van Praag, H. et al. Functional neurogenesis in the adult hippocampus. *Nature* **415**, 1030-4 (2002).
4. Ge, S., Yang, C.H., Hsu, K.S., Ming, G.L. & Song, H. A critical period for enhanced synaptic plasticity in newly generated neurons of the adult brain. *Neuron* **54**, 559-66 (2007).
5. Laplagne, D.A. et al. Functional convergence of neurons generated in the developing and adult hippocampus. *PLoS Biol* **4**, e409 (2006).
6. Carlen, M. et al. Functional integration of adult-born neurons. *Curr Biol* **12**, 606-8 (2002).
7. Schmidt-Hieber, C., Jonas, P. & Bischofberger, J. Enhanced synaptic plasticity in newly generated granule cells of the adult hippocampus. *Nature* **429**, 184-7 (2004).
8. Ge, S., Sailor, K.A., Ming, G.L. & Song, H. Synaptic integration and plasticity of new neurons in the adult hippocampus. *J Physiol* (2008).
9. Carleton, A., Petreanu, L.T., Lansford, R., Alvarez-Buylla, A. & Lledo, P.M. Becoming a new neuron in the adult olfactory bulb. *Nat Neurosci* **6**, 507-18 (2003).
10. Jessberger, S. & Kempermann, G. Adult-born hippocampal neurons mature into activity-dependent responsiveness. *Eur J Neurosci* **18**, 2707-12 (2003).
11. Abrous, D.N., Koehl, M. & Le Moal, M. Adult neurogenesis: from precursors to network and physiology. *Physiol Rev* **85**, 523-69 (2005).
12. Arlotta, P., Magavi, S.S. & Macklis, J.D. Induction of adult neurogenesis: molecular manipulation of neural precursors in situ. *Ann N Y Acad Sci* **991**, 229-36 (2003).
13. Kokoeva, M.V., Yin, H. & Flier, J.S. Neurogenesis in the hypothalamus of adult mice: potential role in energy balance. *Science* **310**, 679-83 (2005).
14. Moyse, E. et al. Neurogenesis and neural stem cells in the dorsal vagal complex of adult rat brain: new vistas about autonomic regulations--a review. *Auton Neurosci* **126-127**, 50-8 (2006).
15. de Waele, C., Campos Torres, A., Josset, P. & Vidal, P.P. Evidence for reactive astrocytes in rat vestibular and cochlear nuclei following unilateral inner ear lesion. *Eur J Neurosci* **8**, 2006-18 (1996).
16. Campos Torres, A., Vidal, P.P. & de Waele, C. Evidence for a microglial reaction within the vestibular and cochlear nuclei following inner ear lesion in the rat. *Neuroscience* **92**, 1475-90 (1999).
17. Tighilet, B., Brezun, J.M., Sylvie, G.D., Gaubert, C. & Lacour, M. New neurons in the vestibular nuclei complex after unilateral vestibular neurectomy in the adult cat. *Eur J Neurosci* **25**, 47-58 (2007).
18. Holstein, G.R. Inhibitory amino acid transmitters in the vestibular nuclei. in *Neurochemistry of the Vestibular System* (eds. Beitz, A.J. & Anderson, J.H.) 143-162 (CRC Press, Florida, 2000).
19. Lacour, M. Restoration of vestibular function: basic aspects and practical advances for rehabilitation. *Curr Med Res Opin* **22**, 1651-9 (2006).
20. West, M.J., Slomianka, L. & Gundersen, H.J. Unbiased stereological estimation of the total number of neurons in thesubdivisions of the rat hippocampus using the optical fractionator. *Anat Rec* **231**, 482-97 (1991).
21. Wilson, V.J. & Melvill Jones, G. *Mammallian Vestibular Physiology*, (New York

London, 1979).
22. Darlington, C.L. & Smith, P.F. Molecular mechanisms of recovery from vestibular damage in mammals: recent advances. *Prog Neurobiol* **62**, 313-25 (2000).
23. Paterson, J.M. et al. Changes in protein expression in the rat medial vestibular nuclei during vestibular compensation. *J Physiol* **575**, 777-88 (2006).
24. Gacek, R.R., Khetarpal, U. & Schoonmaker, J. Morphological and neurochemical correlates of vestibular compensation. *Auris Nasus Larynx* **25**, 193-201 (1998).
25. Dieringer, N. 'Vestibular compensation': neural plasticity and its relations to functional recovery after labyrinthine lesions in frogs and other vertebrates. *Prog Neurobiol* **46**, 97-129 (1995).
26. Bolger, C., Sansom, A.J., Smith, P.F. & Darlington, C.L. An antisense oligonucleotide to brain-derived neurotrophic factor delays postural compensation following unilateral labyrinthectomy in guinea pig. *Neuroreport* **10**, 1485-8 (1999).
27. Tighilet, B., Gustave Dit Duflo, S., Gaubert, C. & Lacour, M. Role of the Neurotrophins in Vestibular Compensation in the cat. in *Abstracts Barany Society XXIII international congress in J Vestib Res* Vol. 14 95-294 (2004).
28. Pencea, V., Bingaman, K.D., Wiegand, S.J. & Luskin, M.B. Infusion of brain-derived neurotrophic factor into the lateral ventricle of the adult rat leads to new neurons in the parenchyma of the striatum, septum, thalamus, and hypothalamus. *J Neurosci* **21**, 6706-17 (2001).
29. Gliddon, C.M., Darlington, C.L. & Smith, P.F. Effects of chronic infusion of a GABAA receptor agonist or antagonist into the vestibular nuclear complex on vestibular compensation in the guinea pig. *J Pharmacol Exp Ther* **313**, 1126-35 (2005).
30. Curthoys, I.S., Smith, P.F. & Darlington, C.L. Postural compensation in the guinea pig following unilateral labyrinthectomy. *Prog Brain Res* **76**, 375-84 (1988).
31. Mori, T., Buffo, A. & Gotz, M. The novel roles of glial cells revisited: the contribution of radial glia and astrocytes to neurogenesis. *Curr Top Dev Biol* **69**, 67-99 (2005).
32. Lafon-Cazal, M. et al. Proteomic analysis of astrocytic secretion in the mouse. Comparison with the cerebrospinal fluid proteome. *J Biol Chem* **278**, 24438-48 (2003).
33. Volterra, A. & Meldolesi, J. Astrocytes, from brain glue to communication elements: the revolution continues. *Nat Rev Neurosci* **6**, 626-40 (2005).
34. Buffo, A. et al. Origin and progeny of reactive gliosis: A source of multipotent cells in the injured brain. *Proc Natl Acad Sci U S A* **105**, 3581-6 (2008).
35. Svensson, M., Eriksson, N.P. & Aldskogius, H. Evidence for activation of astrocytes via reactive microglial cells following hypoglossal nerve transection. *J Neurosci Res* **35**, 373-81 (1993).
36. Campos-Torres, A., Touret, M., Vidal, P.P., Barnum, S. & de Waele, C. The differential response of astrocytes within the vestibular and cochlear nuclei following unilateral labyrinthectomy or vestibular afferent activity blockade by transtympanic tetrodotoxin injection in the rat. *Neuroscience* **130**, 853-65 (2005).
37. Seri, B., Garcia-Verdugo, J.M., McEwen, B.S. & Alvarez-Buylla, A. Astrocytes give rise to new neurons in the adult mammalian hippocampus. *J Neurosci* **21**, 7153-60 (2001).
38. Graeber, M.B., Tetzlaff, W., Streit, W.J. & Kreutzberg, G.W. Microglial cells but not astrocytes undergo mitosis following rat facial nerve axotomy. *Neurosci Lett* **85**, 317-21 (1988).

39. Svensson, M., Mattsson, P. & Aldskogius, H. A bromodeoxyuridine labelling study of proliferating cells in the brainstem following hypoglossal nerve transection. *J Anat* **185 (Pt 3)**, 537-42 (1994).
40. Tighilet, B. & Lacour, M. Gamma amino butyric acid (GABA) immunoreactivity in the vestibular nuclei of normal and unilateral vestibular neurectomized cats. *Eur J Neurosci* **13**, 2255-67 (2001).
41. Gliddon, C.M., Darlington, C.L. & Smith, P.F. GABAergic systems in the vestibular nucleus and their contribution to vestibular compensation. *Prog Neurobiol* **75**, 53-81 (2005).
42. Represa, A. & Ben-Ari, Y. Trophic actions of GABA on neuronal development. *Trends Neurosci* **28**, 278-83 (2005).
43. Bordey, A. Enigmatic GABAergic networks in adult neurogenic zones. *Brain Res Rev* **53**, 124-34 (2007).
44. Stewart, R.R., Hoge, G.J., Zigova, T. & Luskin, M.B. Neural progenitor cells of the neonatal rat anterior subventricular zone express functional GABA(A) receptors. *J Neurobiol* **50**, 305-22 (2002).
45. Tozuka, Y., Fukuda, S., Namba, T., Seki, T. & Hisatsune, T. GABAergic excitation promotes neuronal differentiation in adult hippocampal progenitor cells. *Neuron* **47**, 803-15 (2005).
46. Ge, S. et al. GABA regulates synaptic integration of newly generated neurons in the adult brain. *Nature* **439**, 589-93 (2006).
47. Cameron, S.A. & Dutia, M.B. Cellular basis of vestibular compensation: changes in intrinsic excitability of MVN neurones. *Neuroreport* **8**, 2595-9 (1997).
48. Ge, S., Pradhan, D.A., Ming, G.L. & Song, H. GABA sets the tempo for activity-dependent adult neurogenesis. *Trends Neurosci* **30**, 1-8 (2007).
49. Yuan, T.F. GABA effects on neurogenesis: an arsenal of regulation. *Sci Signal* **1**, jc1 (2008).
50. Lacour, M., Roll, J.P. & Appaix, M. Modifications and development of spinal reflexes in the alert baboon (Papio papio) following an unilateral vestibular neurotomy. *Brain Res* **113**, 255-69 (1976).

Acknowledgments

The authors thank Dr Marie-Pierre Blanchard for technical assistance in confocal imaging and Valerie Gilbert and Catherine Marra for taking care of the animals. This study was supported by grants from the Ministère de l'enseignement supérieur et de la recherche and CNRS (UMR Université de Provence/CNRS N°6149).

LEGENDS OF THE FIGURES

Figure 1 Vestibular nerve section induced a strong increase in the number of BrdU-immunoreactive cells in the deafferented VN. (**a**) Illustration of BrdU immunoreactivity in the medial vestibular nucleus (MVN) in a representative control cat and in three experimental animals infused with AraC or NaCl at different times after unilateral vestibular neurectomy (UVN). Note that vestibular nerve section induced a strong increase in the number of BrdU-immunoreactive cells in the deafferented MVN under an early (UVN/NaCl $D_{0\text{-}30}$) or a delayed AraC (UVN/AraC $D_{20\text{-}50}$) infusion in the fourth ventricle. A lack of BrdU-Ir cells was observed in the MVN of both control cats and cats under an early infusion of AraC (UVN/AraC $D_{0\text{-}30}$). (**b**) Quantitative evaluation of the effects of different conditions of AraC or NaCl infusions (early versus delayed) in the vestibular-neurectomized cats on BrdU-immunoreactive cells in the deafferented vestibular nuclei. Data are mean values (± s.e.m.) of the number of BrdU-immunoreactive cells in the deafferented vestibular nuclei of control cats and unilateral-neurectomized cats infused with an early (UVN/NaCl $D_{0\text{-}30}$ and UVN/AraC $D_{0\text{-}30}$) or a delayed (UVN/NaCl $D_{20\text{-}50}$ and UVN/AraC $D_{20\text{-}50}$) AraC or NaCl infusion in the fourth ventricle. Only values recorded on the lesioned side are illustrated. Data from both sides of control cats were pooled to provide a direct comparison with the subgroups of UVN cats. $*P = 0.0001$ versus control and UVN/AraC $D_{0\text{-}30}$. (AraC: cytosine-ß-D arabinofuranoside; NaCl: sodium chloride; UVN: unilateral vestibular neurectomy; MVN: medial vestibular nucleus; IVN: inferior vestibular nucleus; LVN: lateral vestibular nucleus; SVN: superior vestibular nucleus; D: day). Scale bar: 50 μm and $n = 4$ animals per group.

Figure 2 The subventricular zone (SVZ) is known as a zone of continuous neurogenesis. (**a**) Illustration of BrdU immunoreactivity in the SVZ in a representative control cat and in three

experimental cats infused with AraC or NaCl at different times after unilateral vestibular neurectomy. Note that vestibular nerve section had no effect on the number of BrdU-immunoreactive cells in the subventricular zone whatever the experimental groups. (**b**) Quantitative evaluation of the effects of different conditions of AraC or NaCl infusions (early versus delayed) in the vestibular-neurectomized cats on BrdU-immunoreactive cells in the subventricular zone. Data are mean values (± s.e.m.) of the number of BrdU-immunoreactive cells in the subventricular zone of the different groups of cats. (AraC: cytosine-ß-D arabinofuranoside; NaCl: sodium chloride; UVN: unilateral vestibular neurectomy; D: day). Scale bar: 50 μm and n = 4 animals per group.

Figure 3 Nerve section give rise to a strong glial cell reaction in the vicinity of the lesion. (**a**) Illustration of glial fibrillary acidic protein (GFAP) immunoreactivity in the medial vestibular nucleus (MVN) in a representative control cat and in three experimental animals infused with AraC or NaCl at different times after unilateral vestibular neurectomy. Vestibular nerve section induced a strong increase in the number of GFAP-immunoreactive cells in the deafferented MVN in all groups submitted to UVN. (**b**) Quantitative evaluation of the effects of different conditions of AraC or NaCl infusions (early versus delayed) in the vestibular-neurectomized cats on GFAP-immunoreactive cells in the deafferented vestibular nuclei. Data are mean values (± s.e.m.) of the number of GFAP-immunoreactive cells in the deafferented vestibular nuclei of control cats and unilateral-neurectomized cats infused with an early (D_{0-30}) or a delayed (D_{20-50}) AraC or NaCl infusion in the fourth ventricle. Only values recorded on the lesioned side are illustrated. Data from both sides of control cats were pooled to provide a direct comparison with the subgroups of UVN cats. *P = 0.0001 versus control; ^{+}P = 0.0001 versus UVN/AraC D_{0-30}. (AraC: cytosine-ß-D arabinofuranoside; NaCl: sodium chloride; UVN: unilateral vestibular neurectomy; MVN: medial vestibular nucleus; IVN:

inferior vestibular nucleus; LVN: lateral vestibular nucleus; SVN: superior vestibular nucleus; D: day). Scale bar: 50 μm and n = 4 animals per group.

Figure 4 Confocal analysis of newly generated glial fibrillary acidic protein (GFAP)-immunoreactive (Ir) cells and glutamate decarboxylase (GAD)-67-immunoreactive (Ir) neurons in the deafferented MVN of cats infused with NaCl (**a, b, c, g, h, i**) or cytosine-ß-D arabinofuranoside (AraC) (**d, e, f, j, k, l**) in the fourth ventricle from day 0 to day 30 after unilateral vestibular neurectomy. The 5-bromo-2'deoxyuridine (BrdU)-immunoreactive nuclei are in red (**b, c, h, i**) and the other markers of differentiation in green: GFAP (**a, c, d, f**) and GAD67 (**g, i, j, l**). Note that cats infused with AraC immediately after vestibular lesion and then during thirty days showed a total blockage of newly generated GAD-Ir neurons (**l**) and GFAP-Ir cells (**f**). Scale bar represent 50 μm and n = 4 animals per group.

Figure 5 GAD67-immunoreactive neurons are expressed in all the vestibular nuclei. (**a**) Illustration of GAD67 immunoreactivity in the medial vestibular nucleus (MVN) in a representative control cat and in three experimental animals infused with AraC or NaCl at different times after unilateral vestibular neurectomy. Note that vestibular nerve section induced a significant increase in the number of GAD67-immunoreactive neurons in the deafferented MVN in all groups submitted to UVN. (**b**) Quantitative evaluation of the effects of different conditions of AraC or NaCl infusions (early versus delayed) in the vestibular-neurectomized cats on GAD67-immunoreactive neurons in the deafferented vestibular nuclei. Data are mean values (± s.e.m.) of the number of GAD67-immunoreactive neurons in the deafferented vestibular nuclei of control cats and unilateral-neurectomized cats infused with an early ($D_{0\text{-}30}$) or a delayed ($D_{20\text{-}50}$) AraC or NaCl infusion in the fourth ventricle. Only values recorded on the lesioned side are illustrated. Data from both sides of control cats were

pooled to provide a direct comparison with the subgroups of UVN cats. *P = 0.0001 versus control; ^{+}P = 0.0001 versus UVN/AraC $D_{0\text{-}30}$. (AraC: cytosine-ß-D arabinofuranoside; NaCl: sodium chloride; UVN: unilateral vestibular neurectomy; MVN: medial vestibular nucleus; IVN: inferior vestibular nucleus; LVN: lateral vestibular nucleus; SVN: superior vestibular nucleus; D: day). Scale bar: 50 μm and n = 4 animals per group.

Figure 6 (**a**) Curves illustrating the time course (on the abscissae) of disappearance of horizontal spontaneous nystagmus (HSN) frequency (on the ordinates) for each group of UVN cats infused with AraC or NaCl at different postoperative times. Each data point represents the mean number of HSN quick phase movements in 10 s for 4 animals (five repeated measures per animal per sampling). Error bars represent s.e.m. (**b**) Curves indicating the mean postoperative development of the support surface in the four groups of cats. These values are delimited by the four legs of the cats standing erect without walking and are measured in cm². Data recorded after vestibular lesion were related to individual references and normalized with respect to the preoperative values referred to unity (1 being close to 50 cm²). Standard errors of the mean are reported as vertical lines.). Note the strong delay in time recovery when AraC is infused just after UVN (UVN/AraC $D_{0\text{-}30}$) as compared to the other groups (86 days instead of 50 days). (**c**) The maximal performance (Max P in percentage) is defined as the highest beam rotation speed that did not lead to a fall on four consecutive crossings and is plotted as a function of the number of experimental training sessions in all the groups of cats. These curves illustrate the training time course for each group of cats before unilateral vestibular neurectomy. The training time course of the non-lesioned AraC group was not affected by the AraC infusion. Standard errors of the mean are reported as vertical lines. (**d**) Mean recovery curves illustrating maximal performance of the cat on the rotating beam, expressed in percent of the preoperative maximal performance (on

the ordinates) as a function of the postoperative time in days (on the abscissae). Note the strong delay in time recovery when AraC is infused just after UVN (UVN/AraC $D_{0\text{-}30}$) as compared to the other groups (146 days instead of 46 days). Standard errors of the mean are reported as vertical lines.

Figure 7 Study design: protocol elaborated for studying the effects of the rotating beam conditioning, the unilateral vestibular neurectomy, and the AraC or NaCl infusions on BrdU-immunoreactive cells in the vestibular nuclei and the subventricular zone and on GFAP-labeled and GAD67-labeled cells in the deafferented vestibular nuclei. (C: cellular study; B: behavioral study; UVN: unilateral vestibular neurectomy; AraC: cytosine-β-D arabinofuranoside).

Table 1 Combination and sequential processing of primary and secondary antibodies used for immunohistochemical and immunofluorescent stainings of BrdU, GFAP, or GAD67.

a

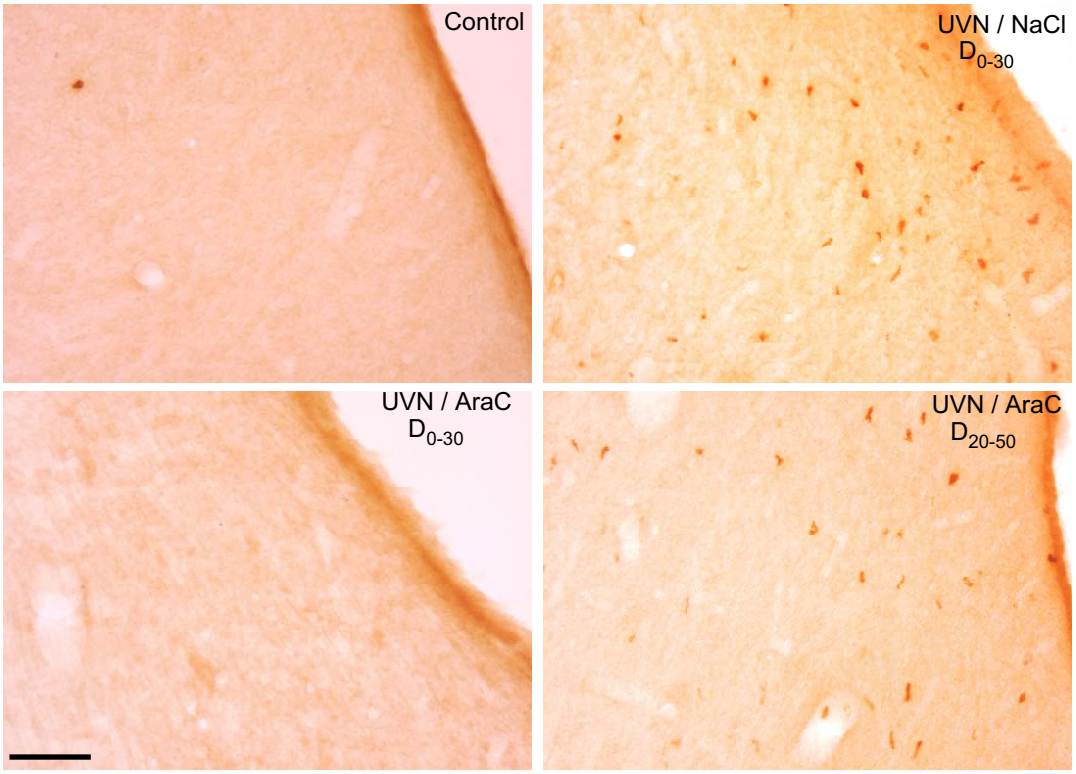
Control
UVN / NaCl
D0-30
UVN / AraC
D0-30
UVN / AraC
D20-50

b

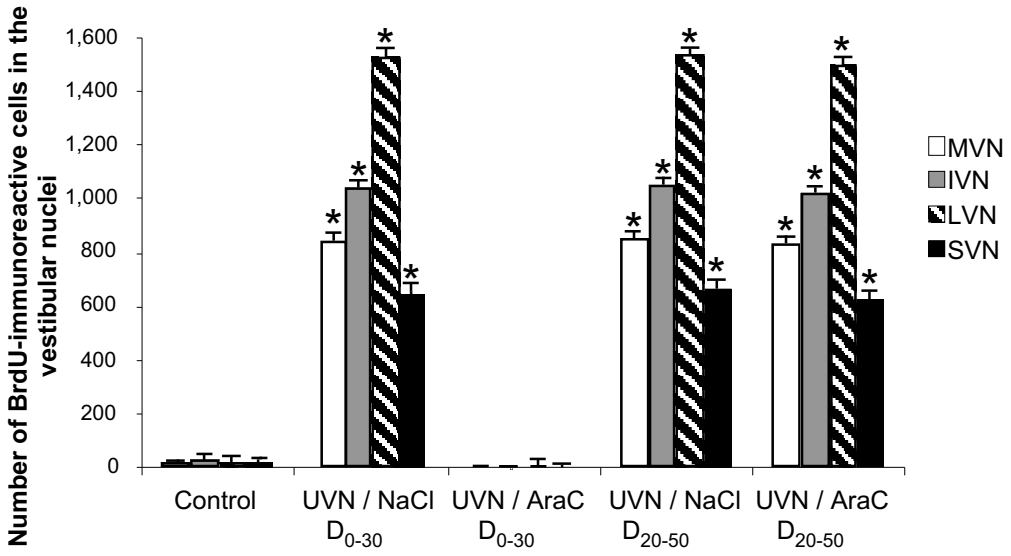
Number of BrdU-immunoreactive cells in the vestibular nuclei
1,600
1,400
1,200
1,000
800
600
400
200
0
Control
UVN / NaCl D0-30
UVN / AraC D0-30
UVN / NaCl D20-50
UVN / AraC D20-50
MVN
IVN
LVN
SVN

a

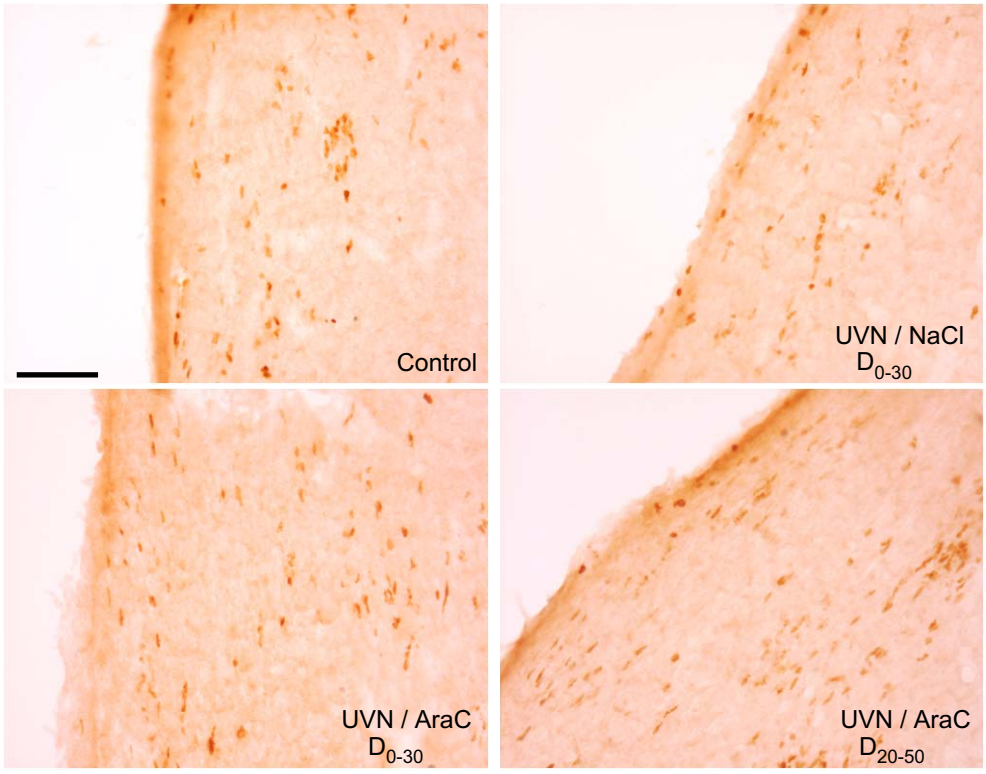
Control
UVN / NaCl
D0-30
UVN / AraC
D0-30
UVN / AraC
D20-50

b

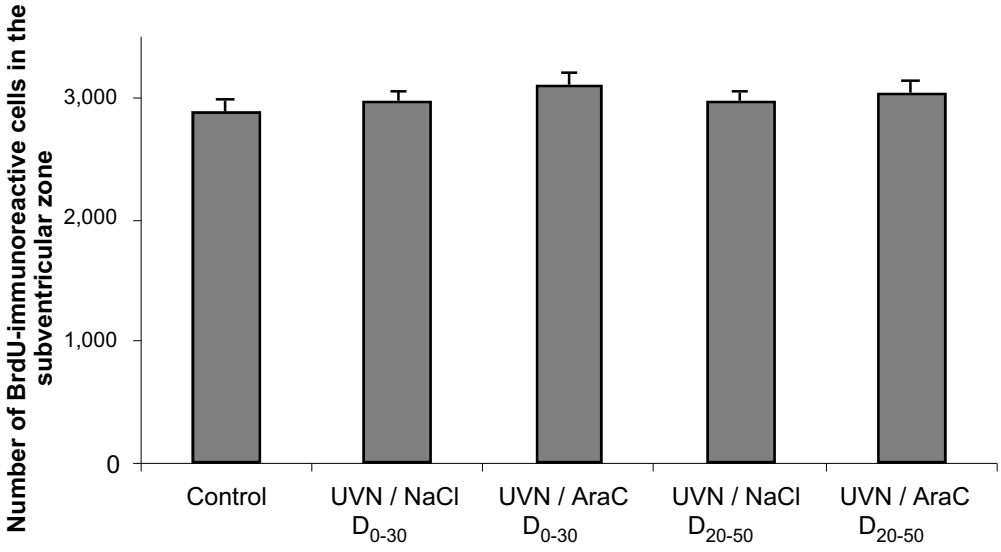
Number of BrdU-immunoreactive cells in the subventricular zone
3,000
2,000
1,000
0
Control
UVN / NaCl
D0-30
UVN / AraC
D0-30
UVN / NaCl
D20-50
UVN / AraC
D20-50

a

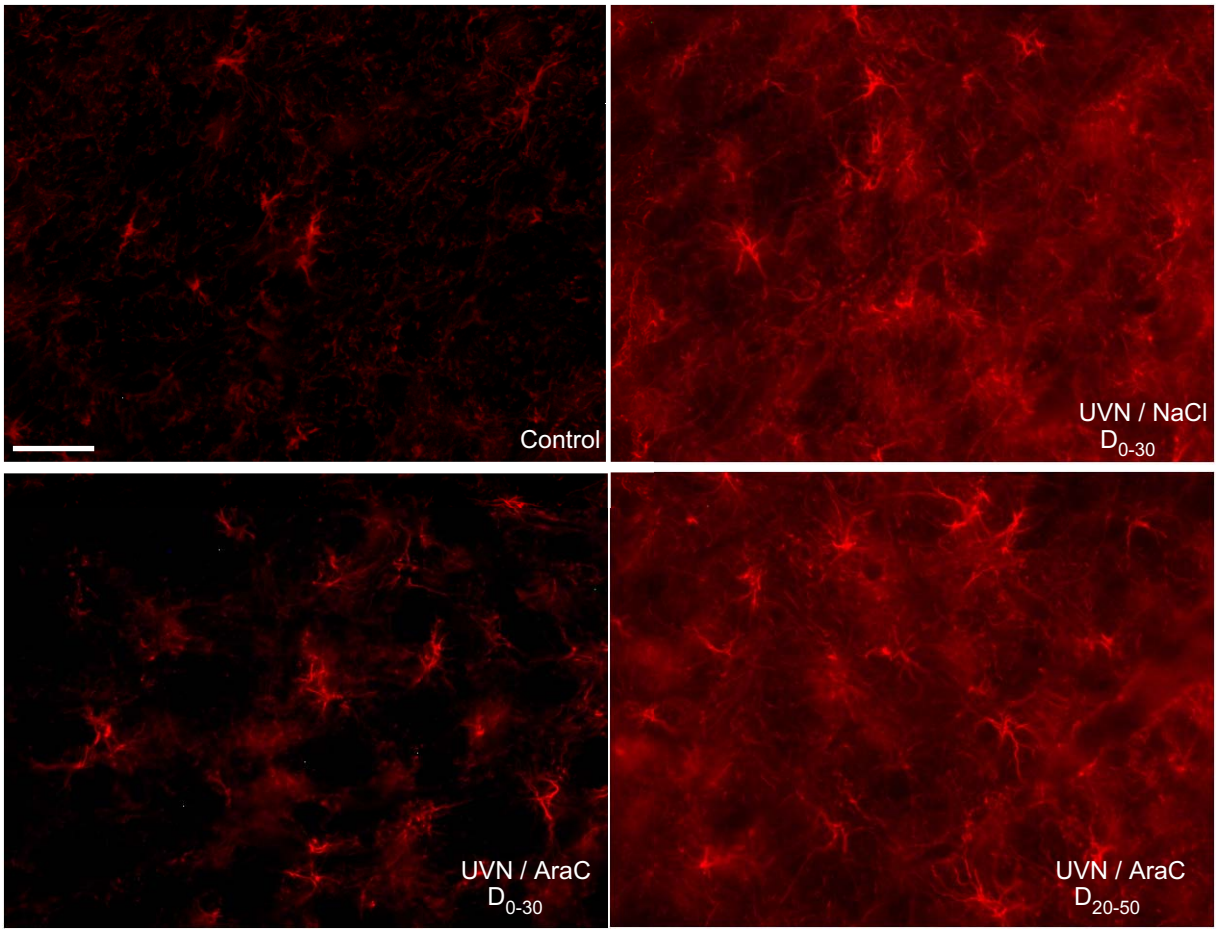
Control
UVN / NaCl
D0-30
UVN / AraC
D0-30
UVN / AraC
D20-50

b

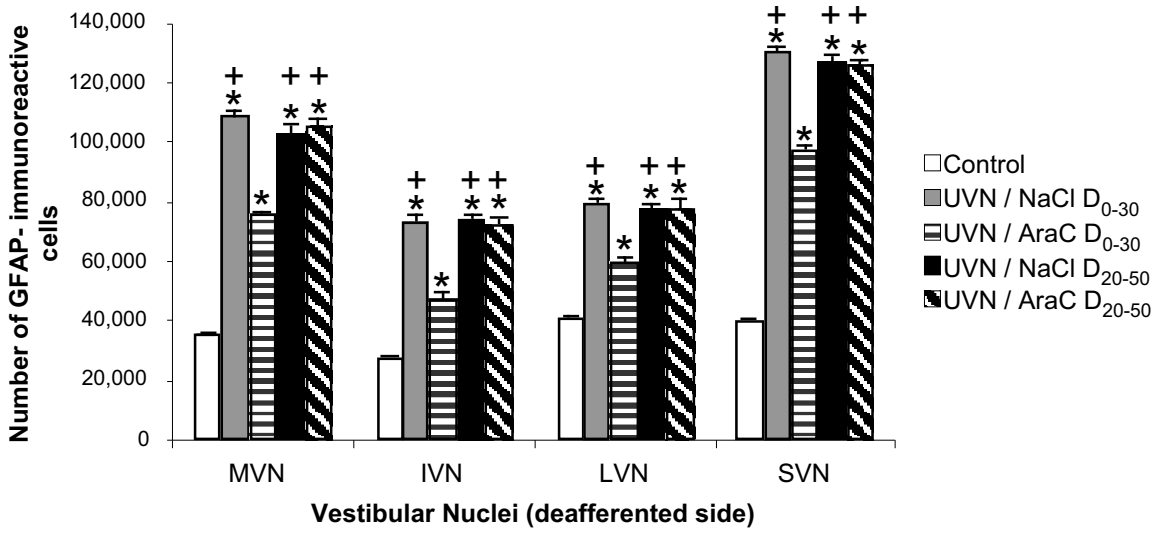
Number of GFAP- immunoreactive cells
140,000
120,000
100,000
80,000
60,000
40,000
20,000
0
MVN
IVN
LVN
SVN
Vestibular Nuclei (deafferented side)
Control
UVN / NaCl D0-30
UVN / AraC D0-30
UVN / NaCl D20-50
UVN / AraC D20-50

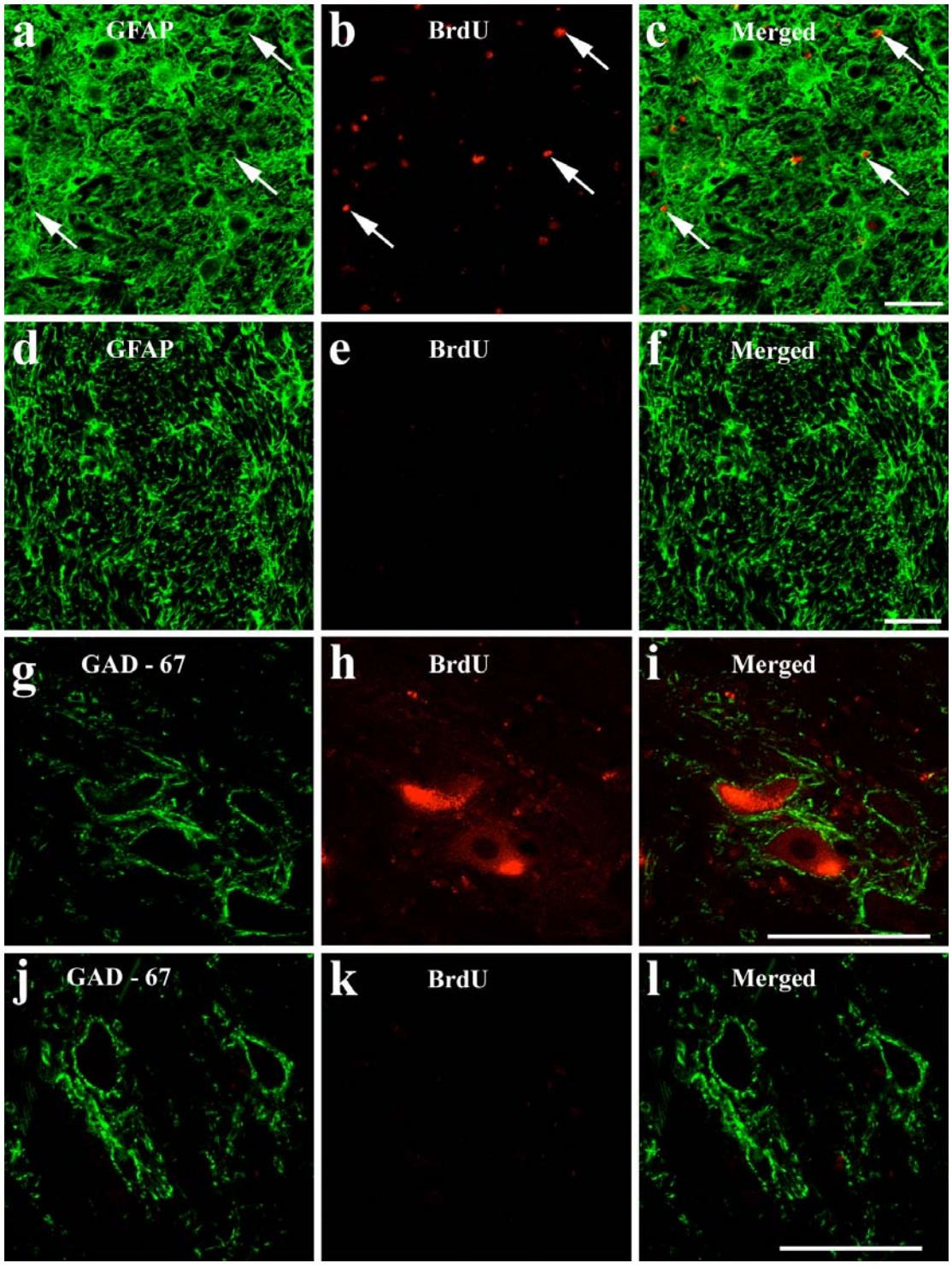
a
GFAP
b
BrdU
c
Merged
d
GFAP
e
BrdU
f
Merged
g
GAD - 67
h
BrdU
i
Merged
j
GAD - 67
k
BrdU
l
Merged

a

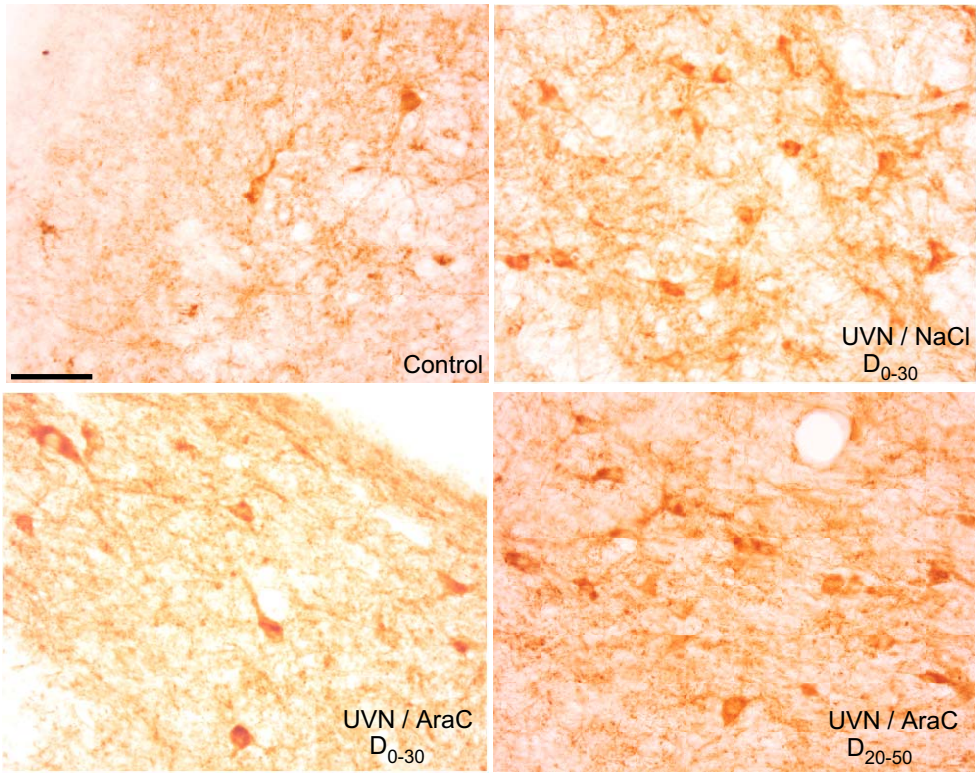
Control
UVN / NaCl
D0-30
UVN / AraC
D0-30
UVN / AraC
D20-50

b

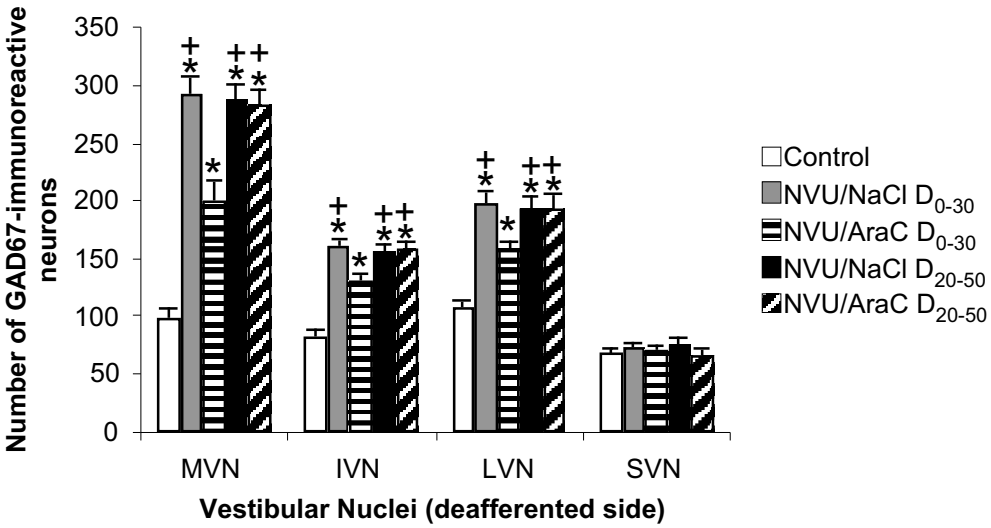
Number of GAD67-immunoreactive neurons
350
300
250
200
150
100
50
0
MVN
IVN
LVN
SVN
Vestibular Nuclei (deafferented side)
Control
NVU/NaCl D0-30
NVU/AraC D0-30
NVU/NaCl D20-50
NVU/AraC D20-50

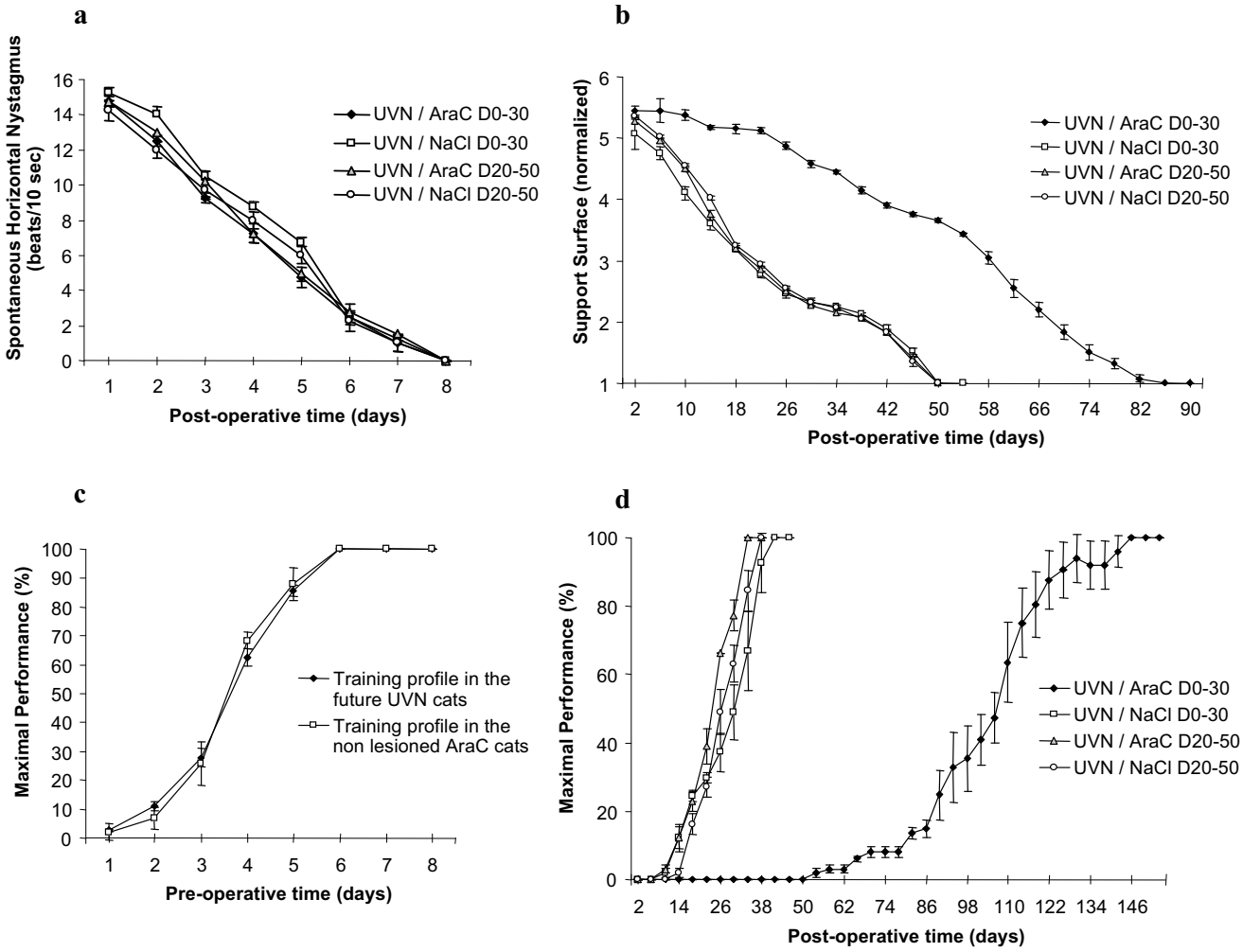
a
Spontaneous Horizontal Nystagmus (beats/10 sec)
Post-operative time (days)
UVN / AraC D0-30
UVN / NaCl D0-30
UVN / AraC D20-50
UVN / NaCl D20-50
b
Support Surface (normalized)
Post-operative time (days)
UVN / AraC D0-30
UVN / NaCl D0-30
UVN / AraC D20-50
UVN / NaCl D20-50
c
Maximal Performance (%)
Pre-operative time (days)
Training profile in the future UVN cats
Training profile in the non lesioned AraC cats
d
Maximal Performance (%)
Post-operative time (days)
UVN / AraC D0-30
UVN / NaCl D0-30
UVN / AraC D20-50
UVN / NaCl D20-50

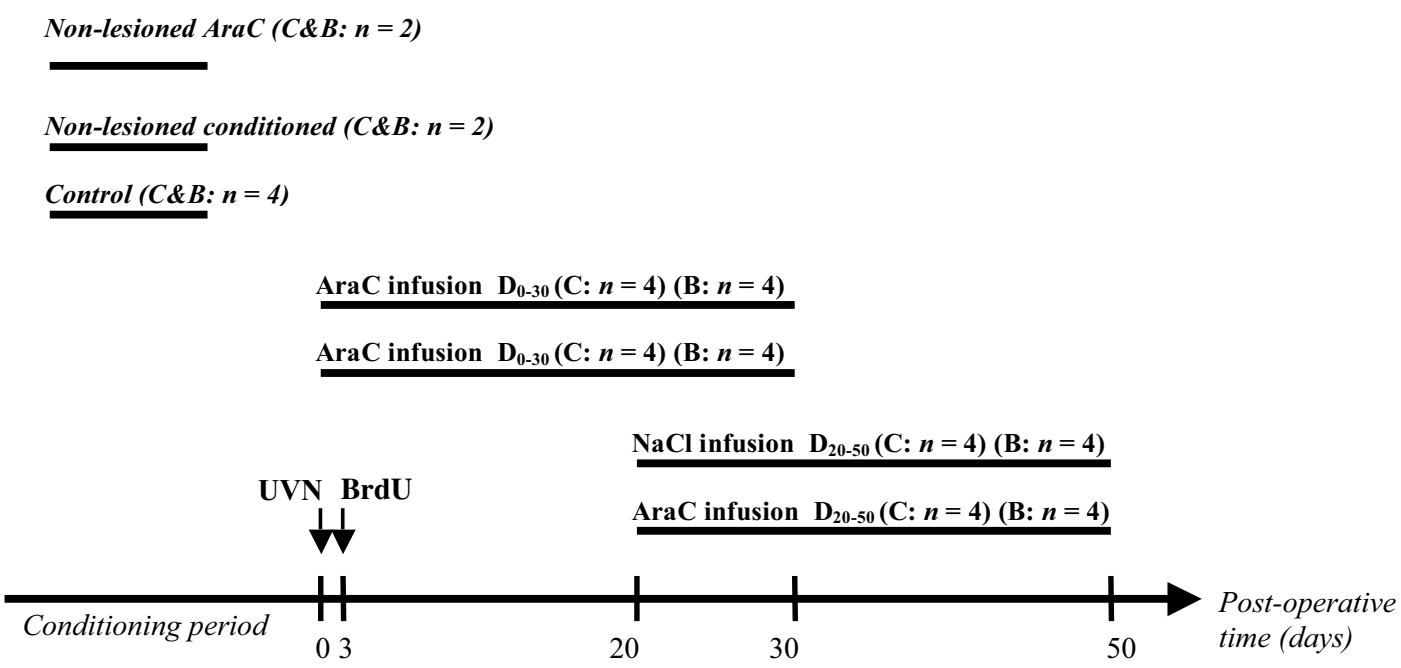
Non-lesioned AraC (C&B: n = 2)
Non-lesioned conditioned (C&B: n = 2)
Control (C&B: n = 4)
AraC infusion D0-30 (C: n = 4) (B: n = 4)
AraC infusion D0-30 (C: n = 4) (B: n = 4)
NaCl infusion D20-50 (C: n = 4) (B: n = 4)
UVN BrdU
AraC infusion D20-50 (C: n = 4) (B: n = 4)
Conditioning period
0 3
20
30
50
Post-operative time (days)

Marker	Primary antibody	Secondary antibody	Technique/coloration
BrdU	Mouse 1 /100, Dako	Horse 1/200, Vector	DAB – brown
GFAP	Rabbit 1/20, Chemicon	Goat 1/200, Vector	DAB – brown
GAD67	Mouse 1/100, Dako	Horse 1/200, Vector	DAB – brown
BrdU	Rat 1/100, Oxford Biot	Rabbit 1/200, Interchim	Alexa 594 - red
GFAP	Rabbit 1/200, Chemicon	Goat 1/200, Interchim	Alexa 488 - green
GAD67	Mouse 1/100, Dako	Rabbit 1/200, Interchim	Alexa 488 - green